

# Cardiomyocyte-Specific Overexpression of Nitric Oxide Synthase 3 Improves Left Ventricular Performance and Reduces Compensatory Hypertrophy After Myocardial Infarction

Stefan Janssens, Peter Pokreisz, Luc Schoonjans, Marijke Pellens, Pieter Vermeersch, Marc Tjwa, Peter Jans, Marielle Scherrer-Crosbie, Michael H. Picard, Zsolt Szelid, Hilde Gillijns, Frans Van de Werf, Desire Collen, Kenneth D. Bloch

**Abstract**—Nitric oxide (NO) is an important modulator of cardiac performance and left ventricular (LV) remodeling after myocardial infarction (MI). We tested the effect of cardiomyocyte-restricted overexpression of one NO synthase isoform, NOS3, on LV remodeling after MI in mice. LV structure and function before and after permanent LAD coronary artery ligation were compared in transgenic mice with cardiomyocyte-restricted NOS3 overexpression (NOS3-TG) and their wild-type littermates (WT). Before MI, systemic hemodynamic measurements, echocardiographic assessment of LV fractional shortening (FS), heart weight, and myocyte width (as assessed histologically) did not differ in NOS3-TG and WT mice. The inotropic response to graded doses of isoproterenol was significantly reduced in NOS3-TG mice. One week after LAD ligation, the infarcted fraction of the LV did not differ in WT and NOS3-TG mice ( $34\pm 4\%$  versus  $36\pm 12\%$ , respectively). Four weeks after MI, however, end-systolic LVID was greater, and fractional shortening and maximum and minimum rates of LV pressure development were less in WT than in NOS3-TG mice. LV weight/body weight ratio was greater in WT than in NOS3-TG mice ( $5.3\pm 0.2$  versus  $4.6\pm 0.5$  mg/g;  $P<0.01$ ). Myocyte width in noninfarcted myocardium was greater in WT than in NOS3-TG mice ( $18.8\pm 2.0$  versus  $16.6\pm 1.6$   $\mu\text{m}$ ;  $P<0.05$ ), whereas fibrosis in noninfarcted myocardium was similar in both genotypes. Cardiomyocyte-restricted overexpression of NOS3 limits LV dysfunction and remodeling after MI, in part by decreasing myocyte hypertrophy in noninfarcted myocardium. (*Circ Res.* 2004;94:1256-1262.)

**Key Words:** nitric oxide synthase ■ myocardial infarction ■ left ventricular remodeling ■ myocyte hypertrophy

After myocardial infarction (MI), left ventricular (LV) remodeling occurs as an adaptive process by which the myocardium changes shape, size, and function in response to increased mechanical and neurohumoral stress. These adaptations include scar maturation and both eccentric and concentric hypertrophy of remote myocardium to compensate for myocardial loss and increase in wall stress.<sup>1</sup> In case of insufficient compensation, LV remodeling becomes maladaptive leading to ventricular dilatation, overt heart failure, and compromised survival.<sup>2</sup>

Nitric oxide (NO) modulates many processes contributing to LV performance including ventricular compliance, myocardial preload and afterload, reperfusion injury,<sup>3–5</sup> and angiogenesis.<sup>6</sup> NO may stimulate new vessel recruitment in ischemic myocardium,<sup>7</sup> reduce excessive myocyte hypertrophy, and limit extracellular matrix deposition and myocardial

fibrosis.<sup>8,9</sup> NO is generated by three NO synthase isoforms, neuronal NOS1, inducible NOS2, and endothelial NOS3. In cardiac myocytes, NOS3 is targeted to caveolae<sup>10,11</sup> where compartmentalization with  $\beta$ -adrenergic receptors and L-type  $\text{Ca}^{2+}$  channels allows NO to inhibit  $\beta$ -adrenergic-induced inotropy.<sup>12</sup> Neuronal NO synthase (NOS1) is localized to cardiac sarcoplasmic reticulum and modulates myocardial contractility via intracellular calcium cycling.<sup>13,14</sup> Increased cardiac NOS1-derived NO production has been suggested to play an important autocrine regulatory role to maintain myocardial contractility after MI in aging rats.<sup>15</sup>

We tested the effect of increased myocardial NOS3 expression on LV remodeling after MI. We compared hemodynamic and echocardiographic parameters of LV performance after MI in transgenic mice with cardiomyocyte-restricted overexpression of human NOS3 (NOS3-TG) and in wild-type (WT)

Original received August 8, 2003; resubmission received December 17, 2003; revised resubmission received March 15, 2004; accepted March 15, 2004. From the Center for Transgene Technology and Gene Therapy (S.J., P.P., M.P., P.V., M.T., P.J., Z.S., H.G., D.C.), Flanders Interuniversity Institute for Biotechnology, the Cardiology Division (S.J., F.V.d.W.), University Hospital Gasthuisberg, University of Leuven, and Thromb-X, LLC (L.S.), Belgium; and the Cardiology Division (M.S.-C., M.H.P., K.D.B.) and Cardiovascular Research Center (M.S.-C., K.D.B.), Massachusetts General Hospital, Harvard Medical School, Boston, Mass.

Correspondence to Stefan Janssens, MD, PhD, Cardiology Division and Center for Transgene Technology and Gene Therapy, University of Leuven, Campus Gasthuisberg, Herestraat 49, B-3000 Leuven, Belgium. E-mail stefan.janssens@med.kuleuven.ac.be

© 2004 American Heart Association, Inc.

Circulation Research is available at <http://www.circresaha.org>

DOI: 10.1161/01.RES.0000126497.38281.23

littermates. We report that after MI, LV function was better preserved in NOS3-TG than in WT mice.

## Materials and Methods

### Experimental Animals

The human cDNA encoding NOS3 was ligated into an expression plasmid containing the  $\alpha$ -myosin heavy chain gene promoter, directing transgene expression in ventricular myocytes.<sup>16</sup> The construct was electroporated together with pPNT, a plasmid containing the neomycin resistance gene, into embryonic stem cells derived from 129/Sv/Ev mice, and neomycin-resistant ES cell clones containing the transgene were identified by PCR. Undifferentiated  $\alpha$ MHC-NOS3 transgenic ES cells were microinjected in Swiss Webster mice, and transgenic offspring were backcrossed for five generations with C57BL/6 mice to obtain a greater than 95% C57BL/6 background. Wild-type littermates were studied as controls.

### In Vitro Analysis of Myocardial NOS3 Overexpression

For details, see the expanded Materials and Methods section in the online data supplement at <http://circres.ahajournals.org>.

### Immunoblot Analysis

To confirm cardiac-selective overexpression of NOS3 in NOS3-TG mice, we adapted the immunoblot protocol reported previously.<sup>17</sup>

### Immunoprecipitation (IP)

For IP, 250  $\mu$ g aliquots of protein extracts from NOS3-TG and WT hearts were incubated overnight in RIPA buffer containing monoclonal anti-human NOS3 antibodies or goat polyclonal anti-CAV3. The extracts precipitated with anti-CAV3 antibodies samples were probed with an anti-human NOS3 monoclonal antibody, and the extracts precipitated with anti-NOS3 antibodies were probed with anti-CAV3 antibodies.

### Immunolocalization and Confocal Analysis

To localize expression of recombinant NOS3 in hearts from transgenic mice, 7- $\mu$ m-thick transverse sections from frozen hearts were immunostained with the monoclonal anti-human NOS3 antibody.

To investigate subcellular localization of the transgene product, isolated cardiomyocytes from adult NOS3-TG and WT mice were prepared and costained with a murine monoclonal antibody recognizing human NOS3 (Becton Dickinson) and a goat polyclonal antibody against caveolin-3 (Santa Cruz, Biotech, USA) or with a rabbit polyclonal antibody recognizing NOS3 (Becton Dickinson) and a murine monoclonal antibody against ryanodine receptor2 (Affinity Bioreagents, UK). Confocal analysis was also performed on 5- $\mu$ m-thick transverse sections from perfusion-fixed and paraffin-embedded hearts using the same antibodies.

### NOS Enzyme Activity and Expression Levels

To measure NOS3 enzyme activity, L-arginine to L-citrulline conversion was assayed in extracts from hearts using a modification of the method described by Xue et al.<sup>18</sup> and Conrad et al.<sup>19</sup>

To evaluate the expression levels of the NOS isoforms in the hearts of transgenic mice, real-time quantitative PCR analysis was performed on RNA samples obtained from six WT and seven NOS3-TG mice using specific probes recognizing sequences complementary to murine genes encoding hypoxanthine phospho-ribosyl transferase (HPRT), NOS1, NOS2, and NOS3. Results were expressed as relative copy numbers standardized to levels of the housekeeping HPRT gene, and the average values in NOS3-TG mice were normalized to the average value in WT mice.<sup>20</sup>

### Analysis of Myocardial Function at Baseline and After Myocardial Infarction

#### Echocardiographic Analysis

Myocardial infarction was produced by ligation of the LAD<sup>21</sup> in 2- to 4-month-old NOS3-TG mice and WT littermates, anesthetized

with pentobarbital (40 to 70 mg/kg IP). Echocardiograms were obtained after urethane anesthesia (1.4 g/kg) before and 7 and 28 days after MI using a 15-MHz linear probe. Measurements of LV end-diastolic and end-systolic diameters and interventricular septum and posterior wall end-diastolic thicknesses at baseline and 4 weeks after MI were performed by three independent observers who were blinded to the experimental group (M.S.-C., M.P., M.T.). All dimensions were normalized to body surface area and fractional shortening (FS) was calculated from the parasternal short- and long-axis views.

### Hemodynamic Measurements at Baseline and After Myocardial Infarction

Hemodynamic measurements of heart rate, blood pressure, and maximal and minimum rates of pressure development ( $dp/dt_{max}$  and  $dp/dt_{min}$ ) were obtained in mice anesthetized with urethane at baseline and 28 days after MI using a 1.4-F high fidelity Millar pressure catheter.

### Response to $\beta$ -Adrenergic Stimulation

In additional NOS3-TG (n=15) and WT (n=11) mice without MI and anesthetized using 2,2,2-tribromoethanol (22  $\mu$ L/g body weight), heart rate, and systolic and diastolic function ( $dp/dt_{max}$  and  $dp/dt_{min}$ ) were measured before and during infusion of isoproterenol (0.1, 0.3, 1.0, 3.0, and 10  $\mu$ L saline).<sup>22</sup>

### Histological Analysis

Twenty-eight days after LAD occlusion, the left ventricle was weighed, fixed with formaldehyde at a perfusion pressure of 100 cm H<sub>2</sub>O, embedded in paraffin, and sectioned along the short axis into 5- and 7- $\mu$ m-thick slices obtained at 1-mm intervals. After staining with hematoxylin-eosin and Sirius red, the infarcted circumference was traced, and the infarcted area was normalized to LV area. Myocyte width was measured in the remote, noninfarcted area of the LV, and measures were obtained at the level of the nucleus in longitudinally sectioned myocytes.<sup>23</sup>

To assess the degree of fibrosis in remote myocardium, a Sirius red and periodic acid Schiff (PAS) histochemical stain was performed on paraffin-embedded sections, and the area of collagen deposition was traced using polarized light and spectral thresholding on a Zeiss Axioplan 2 imaging microscope (Zeiss KS 300 software). The degree of fibrosis was expressed as the area of the remote myocardium containing collagen as a percentage of the total noninfarcted area of the LV surface.

### Statistical Analysis

All data are expressed as mean  $\pm$  SEM unless indicated otherwise. Differences between groups were determined using Student *t* test or 2-way ANOVA for repeated measurements, where indicated. Significant differences were further analyzed using Bonferroni post hoc tests. A value of *P* < 0.05 was considered significant.

## Results

### Selective Myocardial Overexpression of NOS3

#### Immunoblot, Immunoprecipitation, and Confocal Analysis

Abundant NOS3 immunoreactivity was detected in cardiac myocytes of mice carrying the  $\alpha$ MHC-NOS3 transgene (NOS3-TG) but not in those from wild-type (WT) mice (Figure 1A). The intensity and distribution of recombinant NOS3 were comparable in newborn and in 2- to 4-month old NOS3-TG mice (data not shown). Immunoblot analysis confirmed that high concentrations of 135-kDa NOS3 protein were present in hearts of NOS3-TG mice, whereas in WT mice, immunoreactive NOS3 was detectable at low levels (Figure 1B).

To investigate the subcellular localization of the transgene product, immunoprecipitation studies with a caveolin-3-

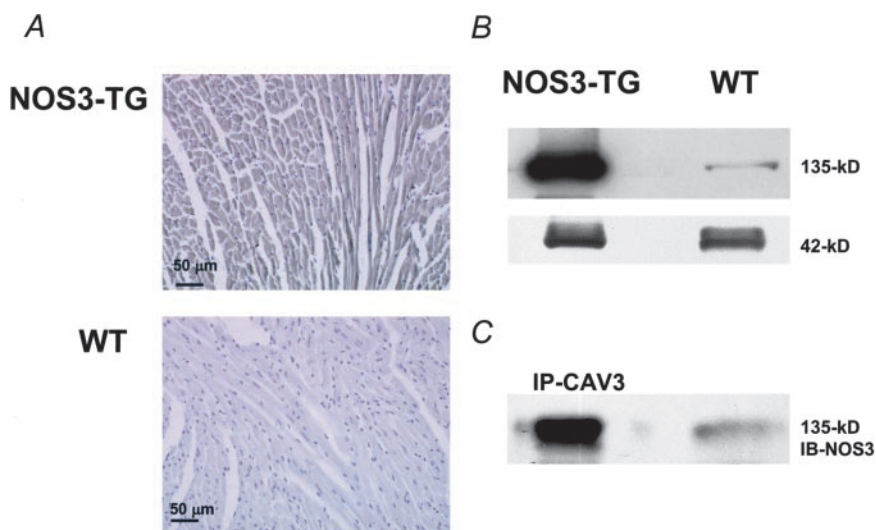


**Figure 1.** Recombinant NOS3 expression in murine heart. A, Representative photomicrograph of NOS3 immunoreactivity in hearts from transgenic mice (NOS3-TG, top) and wild-type mice (WT, bottom) demonstrating increased abundance of NOS3 protein in cardiomyocytes of NOS3-TG compared with WT mice. B, Immunoblot analysis of cardiac extracts from NOS3-TG mice revealed abundant 135-kDa NOS3. Lesser amounts of NOS3 were observed in extracts from WT mice.  $\alpha$ -Actin (42 kDa) is used to control for variability in sample loading. C, Myocardial extracts were immunoprecipitated with anti-caveolin-3 antibodies (IP-CAV3), transferred to nitrocellulose membranes, and probed with antibodies recognizing NOS3 (IB-NOS3). Intensity of the signal was strongly increased in precipitates from transgenic hearts.

specific antibody were performed. Antibody to caveolin-3 coprecipitated NOS in myocardial extracts from WT mice, but the intensity of the signal for NOS3 was strongly increased in precipitates from hearts of NOS3-TG mice (Figure 1C). To further investigate the spatial distribution of endogenous and recombinant NOS3 in wild-type and trans-

genic mice, confocal laser scanning microscopy analysis of isolated adult cardiomyocytes was performed with Alexa Fluor-labeled antibodies against NOS3 (green, Figures 2a and 2d) and caveolin-3 (red, Figures 2b and 2e). The combined image (yellow, Figures 2c and 2f) confirmed the caveolar localization of the transgene product. Additional immuno-

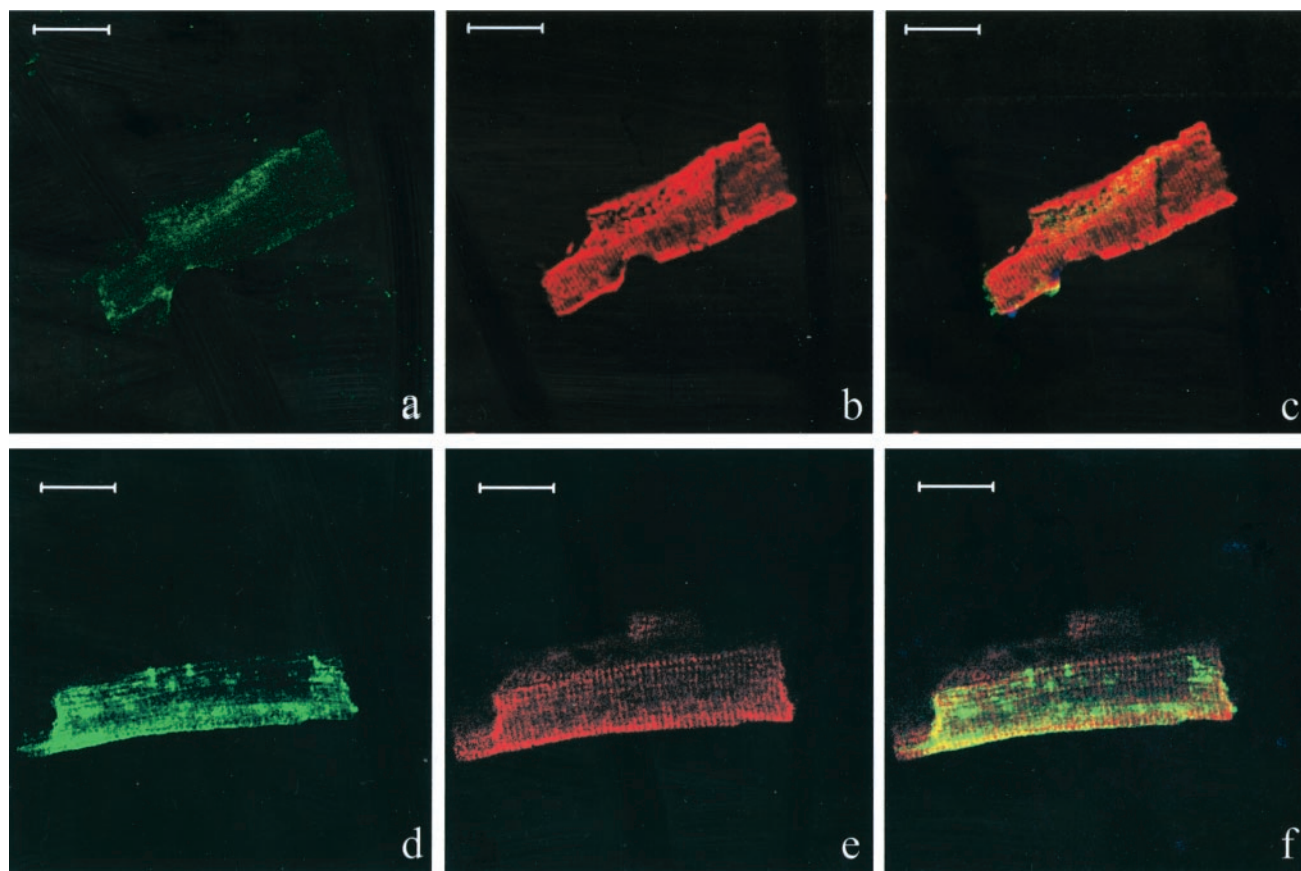


**Figure 2.** Subcellular localization of recombinant NOS3 in isolated adult cardiomyocytes from a WT and NOS3-TG murine heart. Cardiac myocytes from WT (a, b, and c) and NOS3-TG (d, e, and f) were incubated with anti-NOS3 and anti-caveolin-3 antibodies and examined using confocal microscopy. Green areas indicate the presence of NOS3 in WT (a) and NOS3-TG (d). Red areas indicate the presence of caveolin-3 in the same cardiomyocyte in WT and NOS3-TG (b and e, respectively). Yellow areas indicate colocalization of NOS3 with caveolin-3 in WT and NOS3-TG (c and f, respectively). Scale bars=20  $\mu$ m.



**TABLE 1. Relative Copy Numbers of Murine NOS Isoforms in WT and NOS3-TG Mice and Normalized to the Average Value in WT Mice**

	WT (n=6)	NOS3-TG (n=7)	P
mNOS1/HPRT	1±0.29	1.41±0.37	NS
mNOS2/HPRT	1±0.33	1.46±0.27	NS
mNOS3/HPRT	1±0.81	1.09±0.25	NS

Values are mean±SEM. mNOS1 indicates murine neuronal NOS; mNOS2, murine inducible NOS; mNOS3, murine endothelial NOS; HPRT, hypoxanthine ribosyl transferase; and NS, not significant between genotypes.

staining using ryanodine receptor 2 antibodies clearly demonstrated that the transgene product was not localized in the sarcoplasmic reticulum (data not shown). Confocal microscopy of transverse sections confirmed abundant NOS3 expression in NOS3-TG mice but not in WT, and a high degree of targeting to caveolin (see online data supplement).

#### **NOS Enzyme Activity and Expression Levels**

Cardiac extracts from NOS3-TG mice (n=5) contained markedly greater NOS enzyme activity than did extracts from WT mice (n=7), as reflected by an increase in the ability to convert L-arginine to L-citrulline (100±51 versus 3.4±2.9 pmol/mg per min, respectively,  $P<0.05$ ).

To evaluate the impact of the transgene on the expression of the endogenous NOS isoforms, transcript levels of murine NOS1, NOS2, and NOS3, normalized to the constitutive HPRT gene, were compared in NOS3-TG and WT mice (Table 1 and also online data supplement). These results show that cardiomyocyte-specific overexpression of NOS3 does not affect the expression of the other NOS isoforms in the heart.

#### **Analysis of Myocardial Function at Baseline and After Myocardial Infarction**

##### **Echocardiographic and Hemodynamic Measurements at Baseline and After Myocardial Infarction**

Echocardiographic analysis of LV dimensions revealed that end-diastolic and end-systolic diameters, normalized for body surface area, were comparable in NOS3-TG and WT mice, and that computed measurements of fractional shortening, a load-dependent index of systolic function, did not differ

between genotypes (Table 2). At baseline, heart rate, mean blood pressure, and left ventricular systolic and diastolic function did not differ between WT and NOS3-TG mice (Table 3).

To determine whether cardiac-selective NOS3 overexpression could modulate LV remodeling after MI, NOS3-TG and WT mice were subjected to LAD coronary artery occlusion. One week after MI, infarct size was 34±4% (n=7) and 36±12% (n=7) in NOS3-TG and WT mice, respectively. Echocardiographic analysis 28 days after MI revealed significantly smaller end-systolic LV internal diameters in NOS3-TG mice than in WT, consistent with significantly improved LV fractional shortening (Table 2). The favorable LV function profile in NOS3-TG mice 28 days after MI, as assessed by transthoracic echocardiography, was confirmed during cardiac catheterization. Heart rate and mean blood pressure were comparable in NOS3-TG and WT mice (Table 3), whereas indices of LV systolic and diastolic function ( $dP/dt_{max}$  and  $dP/dt_{min}$ ) indicated enhanced contractile performance and ventricular relaxation in NOS3-TG mice.

##### **LV Weight, Myocyte Size, and Myocardial Fibrosis**

Before MI, the LV weight/body weight ratio did not differ in WT and NOS3-TG mice (4.1±0.4 versus 4.2±0.4 in WT, n=10 and NOS3-TG, n=10, respectively). Twenty-eight days after MI, the LV weight/body weight ratio increased in both WT and NOS3-TG mice but was significantly greater in WT than in NOS3-TG mice (Table 3). Before MI, myocyte width in the remote myocardium did not differ between genotypes (10.8±0.8 and 10.8±1.4  $\mu$ m in WT and NOS3-TG mice, respectively), whereas at 28 days after MI, myocyte width was greater in WT than in NOS3-TG mice (Table 3, Figure 3). To investigate whether NOS3 overexpression in the myocardium would attenuate post-MI remodeling by reducing fibrosis in noninfarcted remote myocardium, collagen content of the remote myocardium was measured in tissue sections. In WT and NOS3-TG mice, collagen content in the remote myocardium was 5.3±2.0 and 5.1±2.2% of the total noninfarcted LV area, respectively ( $P=NS$ ).

Finally, to investigate if the favorable hemodynamic profile after MI would translate into a survival benefit in NOS3-TG, we evaluated all cause mortality over the 28 days

**TABLE 2. Echocardiographic Parameters at Baseline and 28 Days After Myocardial Infarction (MI) in Wild-Type (WT) and NOS3 Transgenic Mice (NOS3-TG)**

	WT (Baseline, n=11)	NOS3-TG (Baseline, n=11)	WT (After MI, n=15)	NOS3-TG (After MI, n=15)
BW, g	25±2	23±1	29±1	24±1†
LVID <sub>ED</sub> /BSA, mm/100 cm <sup>2</sup>	3.6±0.2	3.3±0.1	4.6±0.1	4.4±0.1
LVID <sub>ES</sub> /BSA, mm/100 cm <sup>2</sup>	1.7±0.1	1.5±0.1	3.6±0.2	2.9±0.2†
FS, %	51±1	53±2	22±3	34±2†
IVS <sub>ED</sub> /BSA, mm/100 cm <sup>2</sup>	1.3±0.1	1.3±0.1	1.4±0.1	1.4±0.1
PW <sub>ED</sub> /BSA, mm/100 cm <sup>2</sup>	1.1±0.1	1.2±0.1	1.3±0.1	1.3±0.1

Values are mean±SEM. BW indicates body weight; BSA, body surface area measured as  $10.5 \times (BW, g)^{0.67}$ ; LVID<sub>ED</sub>, left ventricular end-diastolic internal diameter; LVID<sub>ES</sub>, left ventricular end-systolic internal diameter; FS, fractional shortening; IVS<sub>ED</sub>, interventricular septum end-diastolic diameter; and PW<sub>ED</sub>, posterior wall end-diastolic diameter. † $P=0.01$  vs WT mice within the same condition (baseline or after MI).

**TABLE 3. Hemodynamic and Histological Parameters at Baseline and 28 Days After Myocardial Infarction (MI) in Wild-Type (WT) and NOS3 Transgenic Mice (NOS3-TG)**

	WT (Baseline, n=7)	NOS3-TG (Baseline, n=7)	WT (After MI, n=20)	NOS3-TG (After MI, n=20)
Heart rate, bpm	610±41	630±39	604±45	603±30
MAP, mm Hg	83±3	79±5	67±6	70±8
dP/dt <sub>max</sub> , mm Hg/s	15 424±3167	14 045±2048	8602±1451	10 784±1350*
dP/dt <sub>min</sub> , mm Hg/s	8639±1924	8110±1028	6234±1078	6950±846*
Remote myocyte width, $\mu$ m	10.8±0.8	10.8±1.4	19.5±1.8	16.7±1.4*
LV/BW, mg/g	4.1±0.4	4.2±0.4	5.6±0.4	4.5±0.6*

Values are mean±SD. MAP indicates mean arterial pressure; dP/dt<sub>max</sub>, maximum rate of developed left ventricular pressure; dP/dt<sub>min</sub>, minimum rate of developed left ventricular pressure; and LV/BW, left ventricular weight/body weight. \* $P<0.05$  vs WT mice after MI.

after LAD occlusion. The majority of deaths occurred in the first week with very few additional deaths beyond 1 week. After 1 month, survival in NOS3-TG mice was 68% versus 58% in WT mice ( $P=NS$ ).

#### Response to $\beta$ -Adrenergic Stimulation

To investigate the impact of transgene expression on the contractile response to  $\beta$ -adrenergic stimulation, five incremental doses of isoproterenol (0.1 to 10 ng) were infused in a separate series of animals to obtain a dose-response curve of left ventricular dP/dt<sub>max</sub>. At baseline, dP/dt<sub>max</sub> in WT and NOS3-TG mice were not different. At doses greater than 1.0 ng isoproterenol, the inotropic response to  $\beta$ -adrenergic stimulation was significantly less in NOS3-TG ( $n=11$ ) than WT mice ( $n=15$ ) (Figure 4). Of interest, although baseline heart rates were comparable in WT and NOS3-TG mice ( $475\pm49$  versus  $478\pm42$  bpm, respectively), they were slower than in our MI protocol, a finding likely attributable to the different anesthetic regimen. The chronotropic response to maximum isoproterenol stimulation, however, was attenuated in NOS3-TG mice ( $504\pm52$  versus  $561\pm42$  bpm in WT;  $P<0.05$ ).

#### Discussion

In the present study, we demonstrated that cardiac-restricted overexpression of endothelial NOS preserves cardiac function and limits deleterious left ventricular remodeling in a

mouse model of myocardial infarction. Recombinant NOS3 was abundantly expressed in cardiomyocytes of transgenic mice and was localized to caveolae, as demonstrated by immunoprecipitation studies and confocal laser scanning microscopy. Increased human NOS3 transcript levels did not affect endogenous expression levels of the constitutive or inducible murine NOS isoforms (Table 1). Despite 30-fold more cardiac NOS enzymatic activity, transgenic mice developed normally and did not differ at baseline from wild-type mice in terms of hemodynamic measurements or echocardiographic measurements of load-dependent indices of systolic function.

Despite similar infarct sizes after LAD ligation in NOS3-TG and WT mice, the former were protected against maladaptive remodeling after MI, as evidenced by a better preserved contractile performance, measured using echocardiography (Table 2). Also residual LV systolic and diastolic function was better preserved in NOS3-TG, as measured invasively (Table 3). Histological analysis demonstrated that LV mass and myocyte width in the noninfarcted remote myocardium were less in NOS3-TG mice (Figure 3), whereas the degree of fibrosis was not different between the two genotypes. These findings suggest that cardiac-specific overexpression of NOS3 attenuated the development of LV remodeling after MI.

Nitric oxide modulates many processes contributing to LV remodeling after MI. The impact of the constitutive NOS

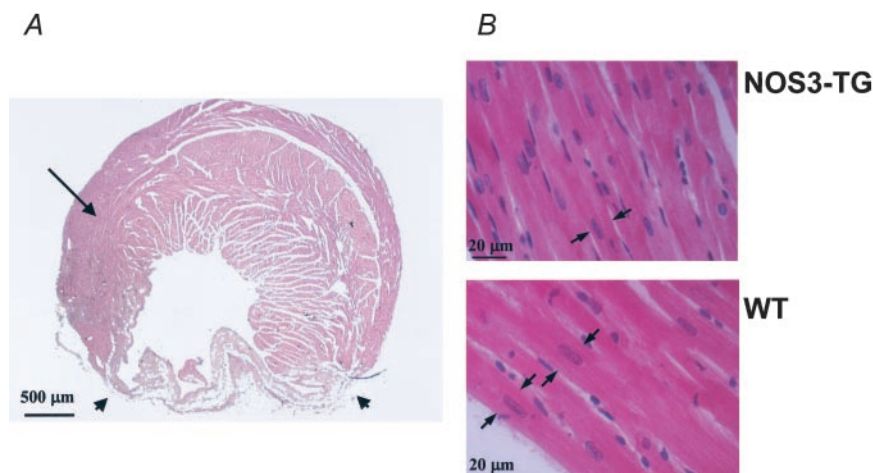


**Figure 3.** Histological analysis of infarcted murine heart. A, Representative transverse section through a WT heart 28 days after MI. Infarct margins are indicated by arrowheads. Remote noninfarcted myocardium is indicated by solid arrow. B, Myocyte width in remote noninfarcted myocardium 1 month after MI in WT and NOS3-TG mice, measured at the level of the nuclei (arrows), is greater in WT than in NOS3-TG.

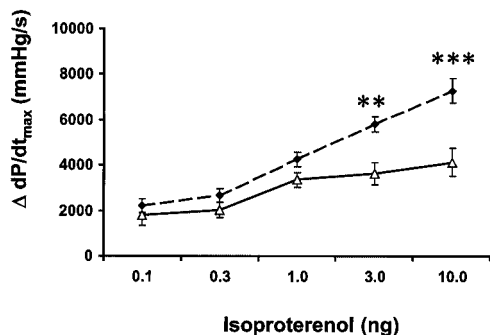


**Figure 4.** Inotropic responses of WT and NOS3-TG mice to  $\beta$ -adrenergic stimulation. Relationship between graded boluses of isoproterenol and changes in contractile function, measured as the maximal rate of intraventricular pressure development ( $dP/dt_{max}$ ) in WT (closed symbols) and NOS3-TG (open symbols) mice. \*\*\* $P < 0.001$ , \*\* $P < 0.01$  vs WT.

isoforms on contractility and calcium cycling has been investigated in isolated cardiomyocytes from mice with targeted deletion of NOS1 and NOS3.<sup>24–26</sup> In addition, left ventricular contractile function after MI has been studied in mice with targeted deletions of NOS3 and NOS2, as well as in transgenic mice with systemic overexpression of NOS3 within the vascular endothelium. NOS3 deficiency was associated with maladaptive remodeling 1 month after MI with increased cardiac hypertrophy and reduced LV function.<sup>23</sup> Others did not find a difference in LV remodeling after large MIs in wild-type and NOS3-deficient mice.<sup>27</sup> The differences in the outcomes of these two studies are likely attributable to differences in the sizes of the MIs studied: in large MIs, the LV remodeling response may reach a maximum obscuring any further deleterious effects of NOS3 deficiency. In the latter study, however, angiotensin-converting enzyme (ACE) inhibitors and angiotensin receptor type-1 ( $AT_1$ ) antagonists were far less effective in preventing myocardial remodeling and preserving LV function after MI in NOS3-deficient mice than in wild-type mice, emphasizing the importance of NOS3 in the salutary effects of these agents. NOS2 deficiency, in contrast, has been reported to be associated with better survival and improved LV function either early<sup>28</sup> or late<sup>29</sup> after MI, although in the latter study the improved contractility was only observed at the highest level of preload in an artificial in vitro system. However, the effect of NOS2-deficiency on LV remodeling after MI may be influenced importantly by the central role of NOS2 in the cardioprotection associated with myocardial ischemia.<sup>30</sup>

The preservation of LV function after MI in our NOS3-TG mice was associated with decreased LV weight and myocyte width. These findings suggest that NOS3-derived NO inhibited myocyte hypertrophy in the remote myocardium in NOS3-TG mice after MI via a paracrine or possibly autocrine mechanism. After MI, a variety of signaling mechanisms stimulate myocyte hypertrophy including the  $\beta$ -adrenergic pathway and the renin angiotensin system.<sup>31</sup> We observed that NOS3-TG mice have a significantly reduced inotropic response to  $\beta$ -adrenergic stimulation (Figure 4). Similarly, Brunner et al<sup>32</sup> reported that the contractile response to norepinephrine was impaired in isolated hearts from mice with cardiac NOS3 overexpression, although

basal contractile function under these experimental conditions was also reduced. Different baseline characteristics most likely reflect different experimental conditions, whereas similar responses to adrenergic stimulation are consistent with the paradigm developed from experiments on isolated cardiomyocytes that endogenous NOS3-derived NO consistently opposes the inotropic response to  $\beta$ -adrenergic stimulation.<sup>33,34</sup> At the same time, chronotropic responses to  $\beta$ -adrenergic stimulation were attenuated in NOS3-TG mice, consistent with a growing consensus that NOS3 in cardiomyocytes reinforces vagal efferent inhibition of heart rate.<sup>35,36</sup> We speculate that the preservation of LV function and attenuation of LV remodeling observed in NOS3-TG mice may, in part, be attributable to inhibition of the ability of  $\beta$ -adrenergic stimuli to induce hypertrophy. At the same time, transgenic mice showed improved diastolic performance after MI, evidenced by the significantly higher rates of LV pressure decline during diastole. Improved systolic and diastolic function may, in turn, decrease the stimulus to remodel after MI.

The protective role of the transgene product on LV remodeling after myocardial infarction did not translate into a survival benefit. In C57BL/6 mice subjected to the same surgical MI model, H. Bayat and colleagues<sup>21</sup> reported LV dilatation and reduced exercise capacity on treadmill testing at 12 to 18 weeks after infarction. Interestingly, and consistent with our findings, mortality occurred only in the early postoperative phase and no additional mortality beyond 2 weeks was reported, even if the animals developed marked congestive heart failure, maladaptive remodeling, and severely impaired left ventricular systolic function 18 weeks after LAD ligation.

We examined whether or not decreased fibrosis in the remote myocardium could contribute to the observed differences in LV contractile function after MI in NOS3-TG and WT mice, but did not find significant differences in collagen deposition using Picrosirius red or PAS stains. It remains to be determined to what extent cardiac-specific NOS3 overexpression modulates the cardiomyocyte apoptosis or myocardial neovascularization, which may also impact LV performance after myocardial infarction.

Recently, S. Jones and colleagues reported that transgenic mice with systemic overexpression of NOS3 within the vascular endothelium had improved survival and decreased pulmonary edema after MI.<sup>37</sup> The benefit in these transgenic mice was attributed to a decrease in LV afterload (and possibly preload), because presence of the transgene was not associated with a beneficial effect on indices of LV remodeling, including cardiac hypertrophy or cardiac contractility. The differences in our findings and those of Jones and colleagues<sup>37</sup> highlight the potential importance of increasing NOS3 expression in cardiomyocytes (rather than in vascular endothelium) to achieve a beneficial impact on LV structure and function after MI.

In summary, cardiomyocyte-restricted overexpression of NOS3 limits LV dysfunction and remodeling after MI, in part by decreasing myocyte hypertrophy in noninfarcted myocardium. Strategies aimed at increasing myocardial NO concentrations such as NOS3 gene transfer (via the coronary arterial or venous circulation) or local (intracoronary or intrapericar-



dial) administration of a slow-release NO donor compound may be promising treatments for LV remodeling after MI.

### Acknowledgments

The research was supported by grants from Bristol-Myers-Squibb (to S.J.) and the National Heart, Lung, and Blood Institute (HL70896 to S.J., M.S.C., M.H.P., and K.D.B.). Dr M. Scherrer-Crosbie was supported by a Scientist Development Grant from the American Heart Association. Dr Janssens is a Clinical Investigator of the Fund for Scientific Research-Flanders and holder of a chair in cardiology sponsored by AstraZeneca.

### References

- Sutton MG, Sharpe N. Left ventricular remodeling after myocardial infarction: pathophysiology and therapy. *Circulation*. 2000;101:2981–2988.
- White HD, Norris RM, Brown MA, Brandt PW, Whitlock RM, Wild CJ. Left ventricular end-systolic volume as the major determinant of survival after recovery from myocardial infarction. *Circulation*. 1987;76:44–51.
- Kupatt C, Hinkel R, Vachenaue R, Horstkotte J, Raake P, Sandner T, Kreuzpointner R, Muller F, Dimmeler S, Feron O, Boekstegers P. VEGF165 transfection decreases postischemic NF- $\kappa$ B-dependent myocardial reperfusion injury in vivo: role of eNOS phosphorylation. *FASEB J*. 2003;17:705–707.
- Gyurko R, Kuhlencordt P, Fishman MC, Huang PL. Modulation of mouse cardiac function in vivo by eNOS and ANP. *Am J Physiol Heart Circ Physiol*. 2000;278:H971–H981.
- Hoshida S, Yamashita N, Igarashi J, Nishida M, Hori M, Kamada T, Kuzuya T, Tada M. Nitric oxide synthase protects the heart against ischemia-reperfusion injury in rabbits. *J Pharmacol Exp Ther*. 1995;274:413–418.
- Zhao X, Lu X, Feng Q. Deficiency in endothelial nitric oxide synthase impairs myocardial angiogenesis. *Am J Physiol Heart Circ Physiol*. 2002;283:H2371–H2378.
- Murohara T, Asahara T, Silver M, Bauters C, Masuda H, Kalka C, Kearney M, Chen D, Symes JF, Fishman MC, Huang PL, Isner JM. Nitric oxide synthase modulates angiogenesis in response to tissue ischemia. *J Clin Invest*. 1998;101:2567–2578.
- Gurjar MV, Sharma RV, Bhalla RC. eNOS gene transfer inhibits smooth muscle cell migration and MMP-2 and MMP-9 activity. *Arterioscler Thromb Vasc Biol*. 1999;19:2871–2877.
- Wang D, Yu X, Brecher P. Nitric oxide and N-acetylcysteine inhibit the activation of mitogen-activated protein kinases by angiotensin II in rat cardiac fibroblasts. *J Biol Chem*. 1998;273:33027–33034.
- Feron O, Dessy C, Opel DJ, Arstall MA, Kelly RA, Michel T. Modulation of the endothelial nitric-oxide synthase-caveolin interaction in cardiac myocytes: implications for the autonomic regulation of heart rate. *J Biol Chem*. 1998;273:30249–30254.
- Ratajczak P, Damy T, Heymes C, Oliviero P, Marotte F, Robidel E, Sercombe R, Boczkowski J, Rappaport L, Samuel JL. Caveolin-1 and -3 dissociations from caveolae to cytosol in the heart during aging and after myocardial infarction in rat. *Cardiovasc Res*. 2003;57:358–369.
- Barouch LA, Harrison RW, Skaf MW, Rosas GO, Cappola TP, Kobeissi ZA, Hobai IA, Lemmon CA, Burnett AL, O'Rourke B, Rodriguez ER, Huang PL, Lima JA, Berkowitz DE, Hare JM. Nitric oxide regulates the heart by spatial confinement of nitric oxide synthase isoforms. *Nature*. 2002;416:337–339.
- Sears CE, Bryant SM, Ashley EA, Lygate CA, Rakovic S, Wallis HL, Neubauer S, Terrar DA, Casadei B. Cardiac neuronal nitric oxide synthase isoform regulates myocardial contraction and calcium handling. *Circ Res*. 2003;92:e52–e59.
- Khan SA, Skaf MW, Harrison RW, Lee K, Minhas KM, Kumar A, Fradley M, Shoukas AA, Berkowitz DE, Hare JM. Nitric oxide regulation of myocardial contractility and calcium cycling: independent impact of neuronal and endothelial nitric oxide synthases. *Circ Res*. 2003;92:1322–1329.
- Damy T, Ratajczak P, Robidel E, Bendall JK, Oliviero P, Boczkowski J, Ebrahimi T, Marotte F, Samuel JL, Heymes C. Up-regulation of cardiac nitric oxide synthase I-derived nitric oxide after myocardial infarction in senescent rats. *FASEB J*. 2003;17:1934–1936.
- Robbins PD, Ghivizzani SC. Viral vectors for gene therapy. *Pharmacol Ther*. 1998;80:35–47.
- Janssens SP, Bloch KD, Nong Z, Gerard RD, Zoldhelyi P, Collen D. Adenoviral-mediated transfer of the human endothelial nitric oxide synthase gene reduces acute hypoxic pulmonary vasoconstriction in rats. *J Clin Invest*. 1996;98:317–324.
- Xue C, Rengasamy A, Le Cras TD, Koberna PA, Dailey GC, Johns RA. Distribution of NOS in normoxic vs. hypoxic rat lung: upregulation of NOS by chronic hypoxia. *Am J Physiol*. 1994;267:L667–L678.
- Conrad KP, Powers RW, Davis AK, Novak J. Citrulline is not the major product using the standard “NOS activity” assay on renal cortical homogenates. *Am J Physiol Regul Integr Comp Physiol*. 2002;282:R303–R310.
- Peirson SN, Butler JN, Foster RG. Experimental validation of novel and conventional approaches to quantitative real-time PCR data analysis. *Nucleic Acids Res*. 2003;31:e73.
- Bayat H, Swaney JS, Ander AN, Dalton N, Kennedy BP, Hammond HK, Roth DM. Progressive heart failure after myocardial infarction in mice. *Basic Res Cardiol*. 2002;97:206–213.
- Hart CY, Burnett JC Jr, Redfield MM. Effects of avertin versus xylazine-ketamine anesthesia on cardiac function in normal mice. *Am J Physiol Heart Circ Physiol*. 2001;281:H1938–H1945.
- Scherrer-Crosbie M, Ullrich R, Bloch KD, Nakajima H, Nasser B, Aretz HT, Lindsey ML, Vancon AC, Huang PL, Lee RT, Zapol WM, Picard MH. Endothelial nitric oxide synthase limits left ventricular remodeling after myocardial infarction in mice. *Circulation*. 2001;104:1286–1291.
- Hare JM. Nitric oxide and excitation-contraction coupling. *J Mol Cell Cardiol*. 2003;35:719–729.
- Barouch LA, Cappola TP, Harrison RW, Crone JK, Rodriguez ER, Burnett AL, Hare JM. Combined loss of neuronal and endothelial nitric oxide synthase causes premature mortality and age-related hypertrophic cardiac remodeling in mice. *J Mol Cell Cardiol*. 2003;35:637–644.
- Ashley EA, Sears CE, Bryant SM, Watkins HC, Casadei B. Cardiac nitric oxide synthase 1 regulates basal and  $\beta$ -adrenergic contractility in murine ventricular myocytes. *Circulation*. 2002;105:3011–3016.
- Liu YH, Xu J, Yang XP, Yang F, Shesely EG, Carretero OA. Effect of ACE inhibitors and angiotensin II type 1 receptor antagonists on endothelial NO synthase knockout mice with heart failure. *Hypertension*. 2002;39:35–42.
- Feng Q, Lu X, Jones D, Shen J, Arnold M. Increased inducible nitric oxide synthase expression contributes to myocardial dysfunction and a higher mortality after myocardial infarction in mice. *Circulation*. 2001;104:700–704.
- Sam F, Sawyer DB, Xie Z, Chang DL, Ngoy S, Brenner DA, Siwik DA, Singh K, Apstein CS, Colucci WS. Mice lacking inducible nitric oxide synthase have improved left ventricular contractile function and reduced apoptotic cell death late after myocardial infarction. *Circ Res*. 2001;89:351–356.
- Bolli R. Cardioprotective function of inducible nitric oxide synthase and role of nitric oxide in myocardial ischemia and preconditioning: an overview of a decade of research. *J Mol Cell Cardiol*. 2001;33:1897–1918.
- Molkentin J, Dorn I. Cytoplasmic signaling pathways that regulate cardiac hypertrophy. *Annu Rev Physiol*. 2001;63:391–426.
- Brunner F, Andrew P, Wolkart G, Zechner R, Mayer B. Myocardial contractile function and heart rate in mice with myocyte-specific overexpression of endothelial nitric oxide synthase. *Circulation*. 2001;104:3097–3102.
- Balligand JL. Regulation of cardiac  $\beta$ -adrenergic response by nitric oxide. *Cardiovasc Res*. 1999;43:607–620.
- Massion PB, Feron O, Dessy C, Balligand JL. Nitric oxide and cardiac function: ten years after, and continuing. *Circ Res*. 2003;93:388–398.
- Balligand JL, Kelly RA, Marsden PA, Smith TW, Michel T. Control of cardiac muscle cell function by an endogenous nitric oxide signaling system. *Proc Natl Acad Sci U S A*. 1993;90:347–351.
- Han X, Kobzik L, Balligand JL, Kelly RA, Smith TW. Nitric oxide synthase (NOS3)-mediated cholinergic modulation of  $\text{Ca}^{2+}$  current in adult rabbit atrioventricular nodal cells. *Circ Res*. 1996;78:998–1008.
- Jones SP, Greer JJ, Van Haperen R, Duncker DJ, De Crom R, Lefer DJ. Endothelial nitric oxide synthase overexpression attenuates congestive heart failure in mice. *Proc Natl Acad Sci U S A*. 2003;100:4891–4896.